A Modified Test Statistic for Maximum-Minimum Eigenvalue Detection Based on Asymptotic Distribution Thresholds

Darren R. Kartchner and Sudharman K. Jayaweera
Communication and Information Sciences Laboratory
Department of Electrical and Computer Engineering
University of New Mexico
Albuquerque, New Mexico, USA.

Abstract—**Signal detection in low-SNR environments is particularly important to the rapidly growing cognitive radio technology. Previous authors have developed detection methods by examining the ratio of the maximum and minimum eigenvalues of the sample covariance matrix. The distribution of this eigenvalue ratio under the null hypothesis is estimated using results from random matrix theory (RMT) to obtain a detection threshold for a Neyman-Pearson test. However, in order to apply asymptotic laws from RMT, the data matrix used to construct the sample covariance matrix must have statistically independent columns, which was not satisfied by test statistics proposed earlier in the literature. This paper considers the case of a data matrix with independent columns to form the test statistic for maximum-minimum eigenvalue (MME) detection, then compares the results with the test statistic as currently defined in literature. The comparison is made with both the semi-asymptotic threshold, which uses the limiting distribution of the maximum eigenvalue and the asymptotic constant to which the minimum eigenvalue converges, as well as the limiting distribution-based threshold, which uses the limiting distribution of the ratio of the maximum and minimum eigenvalues. Simulations compare the expected false alarm rate versus actual false alarm rate, as well as the receiver operating characteristic (ROC) for the following three cases: comparing the two test statistics with the semi-asymptotic threshold, comparing the two test statistics with the limiting distribution threshold, and comparing the two thresholds in conjunction with the newly proposed test statistic. Results demonstrate that the newly proposed test statistic with the limiting distribution threshold is the only case where the actual false alarm rate remains consistently below the false alarm constraint set in the Neyman-Pearson test.**

I. INTRODUCTION

A critical issue in modern communications is efficient spectrum utilization. Under the standard licensing paradigm, only licensed users may access allotted spectrum bands; any duration of time where the licensed user is not using the band is wasted bandwidth. Spectrum sharing is vital in avoiding spectrum waste when spectrum demand grows exponentially. Under spectrum sharing, secondary users are granted access to spectrum bands unused by the primary user and must cede usage of a band when it recognizes that a primary user has started transmission. As such, the spectrum becomes much more dynamic. Cognitive radio technology is used to learn and adapt to the dynamics of a desired section of spectrum [1].

A cognitive radio senses and updates its knowledge about the spectrum based on whether or not it can detect a signal present in the sensed channel or sub-band [2]. Thus, a secondary user utilizing cognitive radio techniques must be able to properly detect signals in order to create an accurate model of the spectrum dynamics and operate effectively.

Detection theory has produced a host of methods to detect a noisy signal. However, in many spectrum sensing situations, there is little to no *a priori* information about the signal or the noise power. In a low-SNR environment, the signal becomes even more difficult to detect. Often, detection algorithms for low-SNR environments tend to leverage the characteristic differences between noise and signals. In particular, maximum-minimum eigenvalue (MME) detection as proposed in [3] utilizes recent findings in random matrix theory (RMT) to characterize the limiting behavior of the eigenvalues of a random matrix to generate a detection threshold.

The detection threshold in [3] is derived with the assumption that the test statistic is formed from a data matrix whose columns are independent and identically distributed (i.i.d.), but such is not the case for the data matrix as currently defined. In this paper, a new test statistic is defined which satisfies this assumption, and it is tested (via simulation) against the previously defined test statistic using the same threshold. While cognitive radio can greatly benefit from improvements to MME detection, these results are also applicable to other fields that draw from detection and estimation theory.

The structure of the paper is as follows: in Section II, the MME test statistic and threshold from [3] are summarized and explained. In Section III, the new test statistic is defined and tested using expected results from RMT. In Section IV, the impact of asymptotic estimation of the minimum eigenvalue is considered for both test statistics, and an additional MME threshold from [4] is defined. The simulations are described in Section V, with accompanying plots of the results. Section VI contains the concluding remarks.

II. PROBLEM FORMULATION AND DEFINITIONS

For a system with a single transmitter and a single receiver, the MME detection scheme proposed in [3] produces an

$L \times L$ sample covariance matrix $\hat{\mathbf{R}}$ from N received samples $x(1) \ldots x(N)$ as follows:

$$\hat{\mathbf{R}} \triangleq \frac{1}{N} \sum_{n=L}^{N+L-1} \mathbf{x}_n \mathbf{x}_n^\dagger \tag{1}$$

where $\mathbf{x}_n \triangleq \begin{bmatrix} x(n) & x(n-1) & \ldots & x(n-L+1) \end{bmatrix}^\top$, $x(i) = 0$ when $i > N$, and $(\cdot)^\dagger$ denotes the transpose or Hermitian transpose, depending on whether the elements of the matrix in question are real or complex, respectively.

The formulation of $\hat{\mathbf{R}}$ in (1) can also be written in terms of an $L \times N$ data matrix $\mathbf{X}$:

$$\hat{\mathbf{R}} = \frac{1}{N} \mathbf{X} \mathbf{X}^\dagger \tag{2}$$

where we let

$$\mathbf{X} \triangleq \begin{bmatrix} \mathbf{x}_L & \mathbf{x}_{L+1} & \ldots & \mathbf{x}_{N+L-1} \end{bmatrix}. \tag{3}$$

The MME detection algorithm leverages the distribution of $\hat{\mathbf{R}}$ under the null hypothesis $\mathcal{H}_0$, corresponding to the received samples consisting of only noise. It is well-known that, if the noise is white and Gaussian, then under $\mathcal{H}_0$, $\hat{\mathbf{R}}$, as defined in (2) will have a Wishart distribution [5], whose spectral characteristics can be used to derive a detection threshold. In particular, the approach of [3] uses the following theorems regarding the limiting distribution and asymptotic values for the maximum and minimum eigenvalues:

Theorem 1a. Assume the following:
- The $L \times L$ sample covariance matrix $\hat{\mathbf{R}}$ has a Wishart distribution with N degrees of freedom (i.e., the data matrix $\mathbf{X}$ is $L \times N$) and scale matrix $\sigma^2 I_L$, where I_L is the $L \times L$ identity matrix.
- L and N increase such that

$$\lim_{N \to \infty} \frac{L}{N} = y$$

where y is a constant that satisfies $0 < y < 1$.

Let $\lambda_{\max}$ be the maximum eigenvalue of $\hat{\mathbf{R}}$. Then $\lim_{N \to \infty} \lambda_{\max} = \frac{\sigma^2}{N} \left(\sqrt{L} + \sqrt{N} \right)^2$ [6].

Theorem 1b. Given the same criteria as Theorem 1a, let $\mu = \left(\sqrt{L} + \sqrt{N} \right)^2$, and $\nu = \left(\sqrt{L} + \sqrt{N} \right) \left(\frac{1}{\sqrt{L}} + \frac{1}{\sqrt{N}} \right)^{\frac{1}{3}}$. Then the probability distribution of $\frac{1}{\nu} \left(\frac{N}{\sigma^2} \lambda_{\max} - \mu \right)$ converges to the Tracy-Widom distribution [7] (of order 1, if the elements of $\mathbf{X}$ are real, or of order 2, if the elements of $\mathbf{X}$ are complex), with probability one [8].

Theorem 2a. Given the same criteria as Theorem 1a, let $\lambda_{\min}$ be the minimum eigenvalue of $\hat{\mathbf{R}}$. Then $\lim_{N \to \infty} \lambda_{\max} = \frac{\sigma^2}{N} \left(\sqrt{L} - \sqrt{N} \right)^2$ [6].

Theorem 2b. Given the same criteria as Theorem 1a, let $\mu' = \left(\sqrt{L} - \sqrt{N} \right)^2$, and $\nu' = \left(\sqrt{L} - \sqrt{N} \right) \left(\frac{1}{\sqrt{L}} - \frac{1}{\sqrt{N}} \right)^{\frac{1}{3}}$. Then the distribution of $\frac{1}{\nu'} \left(\frac{N}{\sigma^2} \lambda_{\min} - \mu' \right)$ converges to the Tracy-Widom distribution (of order 1, if the elements of $\mathbf{X}$ are real, or of order 2, if the elements of $\mathbf{X}$ are complex), with probability one [9].

Based on Theorems 1b and 2a, the following Neyman-Pearson detection threshold was derived [3]:

$$\gamma_{\mathrm{sa}} = \left(\frac{\sqrt{N} + \sqrt{L}}{\sqrt{N} - \sqrt{L}} \right)^2 \times$$
$$\left(1 + \frac{\left(\sqrt{N} + \sqrt{L} \right)^{-\frac{2}{3}}}{(NL)^{\frac{1}{6}}} F_\beta^{-1}(1 - P_{\mathrm{fa}}) \right) \tag{4}$$

where $F_\beta^{-1}(\cdot)$ is the inverse cumulative density function (CDF) of the Tracy-Widom distribution of order β, and P_{fa} is the probability of false alarm constraint on the Neyman-Pearson detector. This threshold will be referred to as the semi-asymptotic MME threshold since it replaces the minimum eigenvalue with its asymptotic value given by Theorem 2a while using the limiting distribution of the maximum eigenvalue from Theorem 1b.

III. PROPOSED NEW TEST STATISTIC

It is known that for $\hat{\mathbf{R}}$ to follow a Wishart distribution, the columns of $\mathbf{X}$ must be i.i.d. [5]. According to the definition of the columns in (1), however, any two adjacent columns overlap by $L - 1$ entries. Hence, the columns of $\mathbf{X}$ are not independent, and therefore, as currently defined, $\hat{\mathbf{R}}$ does not have a Wishart distribution. The incorrect assumption that $\hat{\mathbf{R}}$ has a Wishart distribution may have a negative impact on the expected performance of the MME detector.

We then define a new data matrix $\mathbf{X}'$ and sample covariance matrix $\hat{\mathbf{R}}'$ as follows:

$$\mathbf{X}' \triangleq \begin{bmatrix} \mathbf{x}_L & \mathbf{x}_{2L} & \ldots & \mathbf{x}_{PL} \end{bmatrix}, \tag{5}$$

and

$$\hat{\mathbf{R}}' \triangleq \frac{1}{P} \mathbf{X}' (\mathbf{X}')^\dagger$$
$$= \frac{1}{P} \sum_{n=1}^{P} \mathbf{x}_{nL} \mathbf{x}_{nL}^\dagger \tag{6}$$

where $P = \frac{N}{L}$ is assumed to be an integer. Any two columns of $\mathbf{X}$ are statistically independent when the number of columns between them is at least L (i.e. $\mathbb{E} \left\{ \mathbf{x}_m \mathbf{x}_n^\dagger \right\} = \mathbf{0}_L$ when $|m - n| \geq L$, where $\mathbf{0}_L$ is the $L \times L$ zero matrix). Effectively, $\mathbf{X}'$ is formed from every L-th column of $\mathbf{X}$ to ensure that all columns are independent. Note that for MME detection to function as expected, N and L must be chosen such that $P \geq L$. This ensures that $\hat{\mathbf{R}}'$ is full-rank with probability one [10], which implies that $\lambda_{\min} > 0$ with probability one, and the test statistic is well-defined. Thus, N and L should be selected such that $N \geq L^2$. Furthermore, when applying the results of RMT to $\hat{\mathbf{R}}'$ (i.e. the theorems in this paper and the

derived threshold in (4)), substitute all references to N with P.

Figure 1 illustrates the results of a simulation under two scenarios: when the columns of the data matrix overlap as in (1), and when the columns are independent as in (6). For each case, real samples were used. The empirical distribution of the maximum eigenvalue of the sample covariance matrix was computed, then scaled using the parameters μ and ν in Theorem 1b. As a reference, the Tracy-Widom distribution of order 1 is also plotted. The results show that when using independent columns as proposed above, the scaled distribution of the maximum eigenvalue indeed converges to the Tracy-Widom distribution of order 1, as predicted by Theorem 1b. However, from Fig. 1, it is also clear that when using the overlapping columns as in [3], the scaled distribution does not converge to the Tracy-Widom distribution of order 1.
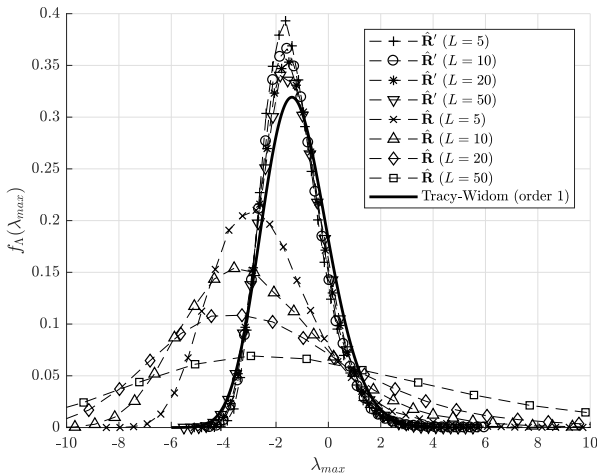
Fig. 1. Empirical distributions of the maximum eigenvalue for $\frac{N}{L} = 10$ and varying values of L, scaled using μ and ν from Theorem 1b, for 25,000 runs. The cases of independent columns ($\hat{\mathbf{R}}'$) and overlapping columns ($\hat{\mathbf{R}}$) are presented, along with the Tracy-Widom distribution of order 1. The scaled distribution in the case of independent columns seems to converge to the Tracy-Widom distribution. The scaled distribution in the case of the overlapping columns has a similar shape, but does not converge in mean or variance to the Tracy-Widom distribution using the scaling factors from Theorem 1b.

IV. THRESHOLD ANALYSIS

Observe that the threshold used in (4) depends on the estimate of the minimum eigenvalue as its asymptotic value, as defined in Theorem 2a. Consider the mean-squared error of this estimate:

$$MSE = \mathbb{E}\left\{ \left(\lambda_{\min} - \hat{\lambda}_{\min} \right)^2 \right\} \tag{7}$$

where $\lambda_{\min}$ is the empirical minimum eigenvalue and $\hat{\lambda}_{\min}$ is the asymptotic value of the minimum eigenvalue as given in Theorem 2a. The MSE is estimated by using Monte Carlo simulation and calculating the sample mean of the squared error between the minimum eigenvalue and the estimate. The ratio $\frac{N}{L} = 100$ is kept constant for each simulation. The cases

of the minimum eigenvalue of $\hat{\mathbf{R}}$ and $\hat{\mathbf{R}}'$ are simulated, and the results are illustrated in Fig. 2. As expected, in the independent columns case, the mean-squared error of the estimate goes to zero as L increases, but the error is not negligible for smaller values of L. Meanwhile, in the case of the overlapping columns, the MSE does not converge to zero.
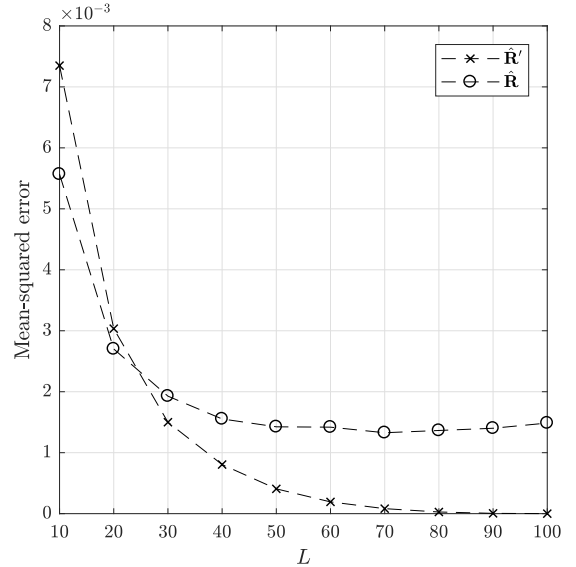
Fig. 2. Mean-squared error of using the asymptotic value for the minimum eigenvalue in Theorem 2a as an estimate for the minimum eigenvalue, for a constant $\frac{N}{L} = 100$. The estimate was made using a Monte Carlo simulation for 10,000 runs. As Theorem 2a suggests, the error goes to 0 as L increases in the case where $\mathbf{X}$ has independent columns. However, the complexity of computing the eigenvalues of $\hat{\mathbf{R}}$ increases on the order of approximately $O(L^3)$, so there is a notable trade-off between complexity and estimation error.

An alternative detection threshold has been derived in [4] using the limiting distribution of $\lambda_{\min}$ from Theorem 2b:

$$\gamma_{\text{ld}} = F_T^{-1}(1 - P_{\text{fa}}) \tag{8}$$

where $F_T^{-1}(\cdot)$ is the inverse CDF corresponding to the limiting distribution of the eigenvalue ratio. This is defined as

$$f_T(t) = I_{\{t>1\}} \int_0^\infty x f_{\lambda_{\max}}(tx) f_{\lambda_{\min}}(x) \, \mathrm{d}x \tag{9}$$

where $I_{\{\cdot\}}$ is the indicator function, and $f_{\lambda_{\max}}(\cdot)$ and $f_{\lambda_{\min}}(\cdot)$ are the Tracy-Widom distribution appropriately scaled using the factors from Theorem 1b and 2b to represent the limiting distributions of the maximum and minimum eigenvalues, respectively. These scaled distributions are defined as

$$f_{\lambda_{\max}}(z) = \frac{1}{\nu} f_\beta \left(\frac{z - \mu}{\nu} \right) \tag{10}$$

and

$$f_{\lambda_{\min}}(z) = -\frac{1}{\nu'} f_\beta \left(\frac{z - \mu'}{\nu'} \right) \tag{11}$$

where $f_\beta(\cdot)$ is the PDF of the Tracy-Widom distribution whose order corresponds to whether the received samples are real

(order 1) or complex (order 2). The threshold in (8) will hereon be referred to as the limiting distribution threshold.

V. SIMULATIONS

The detector performance was measured using two metrics: actual false alarm rate versus expected false alarm rate (i.e., the parameter P_{fa} used in threshold calculation), and the complement of the receiver operating characteristic (ROC) curve. Performance was estimated using Monte Carlo simulation, for 25,000 runs. For all simulations, real samples were used, $L = 20$, and $N = 4000$ (therefore, $P = 200$). Consider the following cases:

Case	Test Statistic	Threshold
1	$\frac{\lambda_{\max}}{\lambda_{\min}}$ of $\hat{\mathbf{R}}$	Semi-asymptotic
2	$\frac{\lambda_{\max}}{\lambda_{\min}}$ of $\hat{\mathbf{R}}'$	Semi-asymptotic
3	$\frac{\lambda_{\max}}{\lambda_{\min}}$ of $\hat{\mathbf{R}}$	Limiting distribution
4	$\frac{\lambda_{\max}}{\lambda_{\min}}$ of $\hat{\mathbf{R}}'$	Limiting distribution
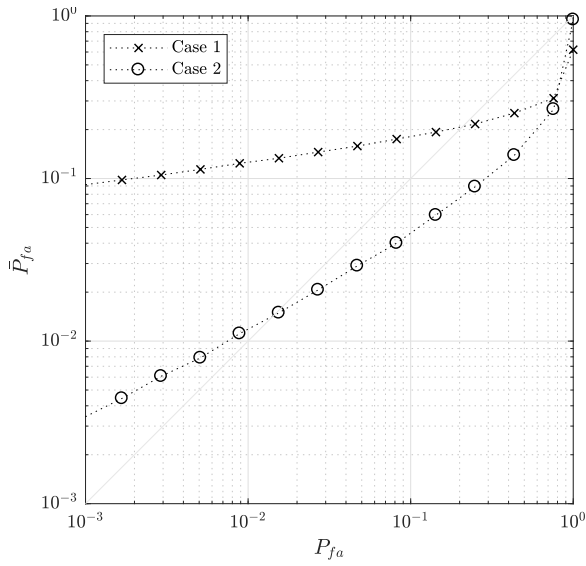
Fig. 3. The expected false alarm rate (P_{fa}) versus the actual false alarm rate ($\bar{P}_{\text{fa}}$) for Cases 1 and 2. In both cases, there are values of $\bar{P}_{\text{fa}}$ which exceed the constraint, but in Case 1, it may exceed the constraint by orders of magnitude. Thus, the Neyman-Pearson test in Case 1 may be highly inaccurate.

For each simulation, three results are compared for the two cases under test. First, the expected false alarm rate (P_{fa}, or the parameter used to define the Neyman-Pearson test) is compared to the empirical false alarm rate, denoted as $\bar{P}_{\text{fa}}$. If $\bar{P}_{\text{fa}} > P_{\text{fa}}$, then the detection probability as a function of false alarm rate (i.e., the ROC) does not provide an accurate assessment of the detection scheme. Second, the complementary ROC curves are plotted, comparing the missed detection rate ($1 - \bar{P}_D$) to P_{fa}. Such curves are often used to characterize a detection scheme, but if $\bar{P}_{\text{fa}}$ exceeds the constraint, then

these curves again may be deceiving. Therefore, the third result plots $1 - \bar{P}_D$ against $\bar{P}_{\text{fa}}$ to give a better idea of how the complementary ROC curves would look if the detection scheme used a theoretical threshold in conjunction with the test statistic such that $\bar{P}_{\text{fa}} = P_{\text{fa}}$. Thus, this result offers insight as to the best-case detection performance for a given test statistic or threshold, as well as a desired P_{fa}.

The first simulation compares Cases 1 and 2 in order to test the newly proposed test statistic against the previously defined test statistic of [3], while using the semi-asymptotic threshold. The results of this simulation are shown in Figs. 3 and 5. Note that in Case 1, for $P_{\text{fa}} < 0.2$, $\bar{P}_{\text{fa}} > P_{\text{fa}}$, sometimes by multiple orders of magnitude (Fig. 3). Thus, upon examining Figs. 5a-b, although $\bar{P}_D$ of Case 1 is higher than that of Case 2 for a given P_{fa}, this comes at the cost of a much higher $\bar{P}_{\text{fa}}$ than that with Case 2. Figures 5c-d demonstrate that, if an ideal threshold is applied with each test statistic, then the overlapping columns case would still have a higher $\bar{P}_D$ for a given P_{fa} than the independent columns case. It is known that detection probability increases for a given P_{fa} as the number of columns of the data matrix increases [3]. As there are $N = 4000$ columns in Case 1, while there are only $P = 200$ columns in Case 2, these results are consistent with the literature. However, since the columns are not independent in Case 1, the derivation of an ideal threshold for the overlapping columns case will be more complex than the thresholds derived for the independent columns case.
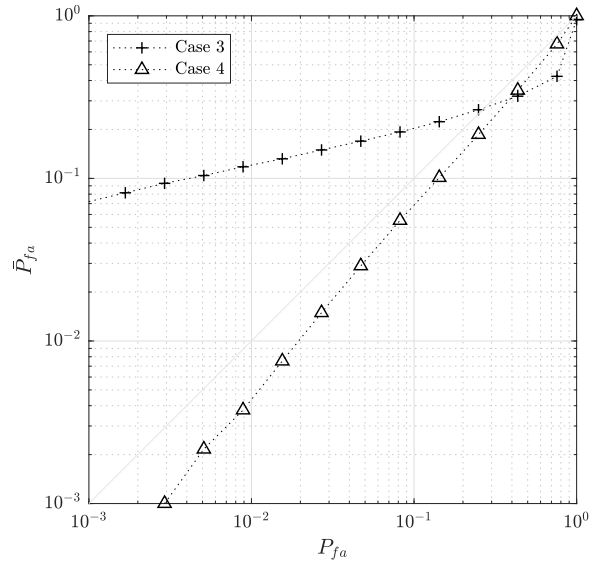
Fig. 4. P_{fa} versus $\bar{P}_{\text{fa}}$ for Cases 3 and 4. Much like the first simulation, $\bar{P}_{\text{fa}}$ may greatly exceed the constraint, meaning the test may not be accurate in Case 3. For Case 4, $\bar{P}_{\text{fa}}$ remains within the constraint for all P_{fa}.

Cases 3 and 4 were tested in the second simulation. The purpose was to verify that the same conclusions can also be drawn when the limiting distribution threshold is used. Figures 4 and 6 display the results. Indeed, the results appear to be similar to those of the first simulation. Namely, Case 3 has a $\bar{P}_{\text{fa}}$ higher than P_{fa} for low values of P_{fa} (Fig. 4), and this
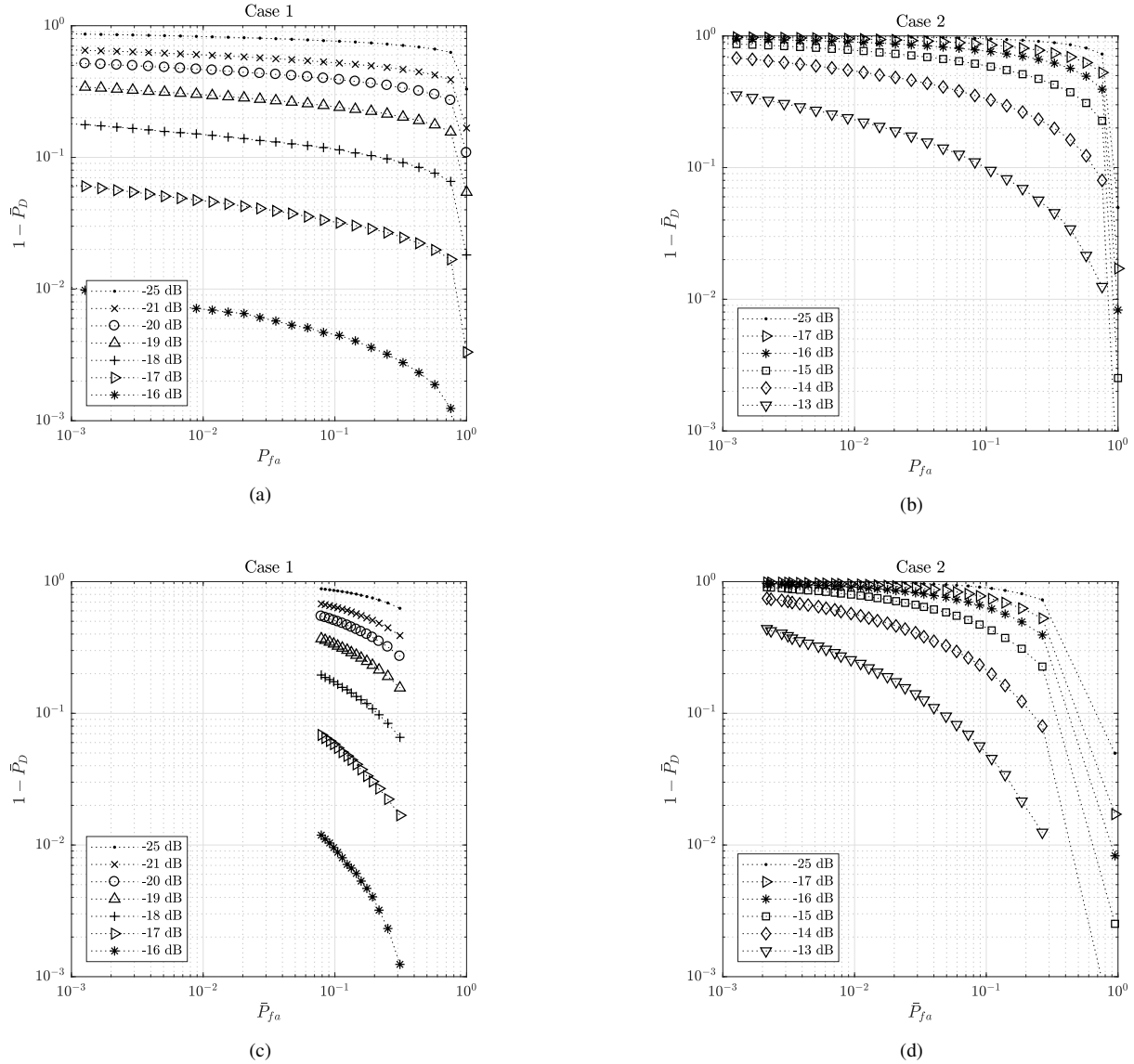
Fig. 5. a) Complementary ROC curves for Case 1. b) Complementary ROC curves for Case 2. c) $1 - \bar{P}_D$ as a function of $\bar{P}_{\text{fa}}$ for Case 1. d) $1 - \bar{P}_D$ as a function of $\bar{P}_{\text{fa}}$ for Case 2. Comparing Figs. 5a and 5b, Case 1 exhibits a higher detection rate than Case 2 because the false alarm rate is also much higher. In the second pair of plots, Case 1 still exhibits a higher detection probability than Case 2, likely because the test statistic in Case 1 is formed from a sample covariance matrix averaged over more data columns than Case 2.

results in a higher detection rate for Case 3 than for Case 4 (Figs. 6a-b). Furthermore, when comparing $1 - P_D$ and $\bar{P}_{\text{fa}}$ for both cases, Case 3 also has a higher detection rate than Case 4 (Figs. 6c-d). Therefore, the results observed from these simulations are not conditional on which MME threshold is used.

The third simulation compares Cases 2 and 4, in order to test the semi-asymptotic threshold versus the limiting distribution threshold when using the independent columns. Figures 7 and 8 record the results of this simulation. From Fig. 7, it is seen that for Case 2, $\bar{P}_{\text{fa}} > P_{\text{fa}}$ for $P_{\text{fa}} < 0.015$, while for Case 4, $\bar{P}_{\text{fa}}$ remains reliably within the constraint. Therefore, for Neyman-Pearson tests that require the false alarm rate to be

bound below a given value, the limiting distribution threshold is desirable over the semi-asymptotic threshold. The complementary ROC curves in Fig. 8 demonstrate that for a given P_{fa}, there is a trade-off between the semi-asymptotic threshold and the limiting distribution threshold at $P_{\text{fa}} \approx 0.05$. Thus, when P_{fa} lies between 0.015 and 0.05, the semi-asymptotic threshold exhibits higher detection rates than the limiting distribution threshold, but when $P_{\text{fa}} > 0.05$, then the limiting distribution threshold has a higher $\bar{P}_D$.

VI. CONCLUSION

MME detection, as initially conceived, defines its test statistic in a way that does not exactly agree with the derived
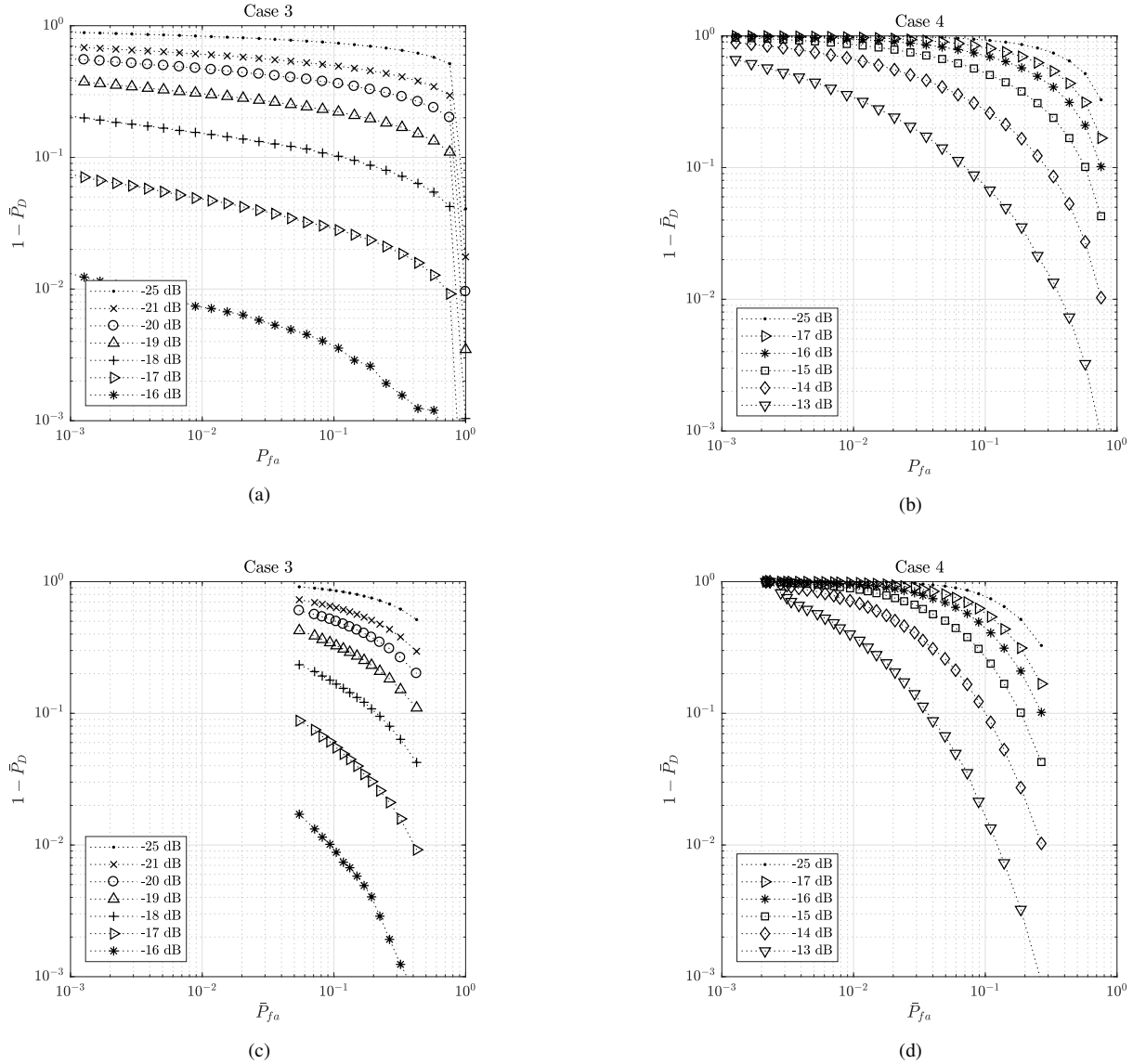
Fig. 6. a) Complementary ROC curves for Case 3. b) Complementary ROC curves for Case 4. c) $1 - \bar{P}_D$ as a function of $\bar{P}_{\text{fa}}$ for Case 3. d) $1 - \bar{P}_D$ as a function of $\bar{P}_{\text{fa}}$ for Case 4. The same conclusions from the first simulation also apply here; therefore, the impact of using independent columns instead of overlapping columns is independent of which threshold is used.

threshold: the constructed sample covariance matrix $\hat{\mathbf{R}}$ will not have a Wishart distribution under the null hypothesis, as was assumed. As a result, the true false alarm rate may greatly exceed the desired false alarm rate, as seen in Figs. 3 and 4. A remedy is to redefine the sample covariance matrix so that no samples are repeated across columns of the data matrix. The trade-off is that for a fixed number of collected samples and a fixed smoothing rate L, the data matrix will have fewer columns, leading to a lower detection rate. Figs. 5c-d and 6c-d demonstrate this trade-off. It should be noted that in recent contributions to MME detection, the $L \times N$ data matrix used for the test statistic is constructed by concatenating N samples collected from L individual receivers [11]. In this case, the test statistic is distributed as originally derived, but

the general derivation in [3] must be modified to guarantee that the columns of the data matrix are independent.

The methods of using independent columns versus overlapping columns are somewhat analogous to Bartlett's method versus Welch's method of calculating the periodogram [12], respectively. Each column of the data matrix is similar to the periodogram window. Bartlett's method uses non-overlapping windows to calculate the periodogram, while Welch's method uses a sliding-window approach, allowing for window-to-window overlap of the data. One of the benefits of using Welch's method is that it averages over more windows given the same amount of data, which is analogous to having more columns in the data matrix used for MME detection. Therefore, there may be merit to using overlapping columns when
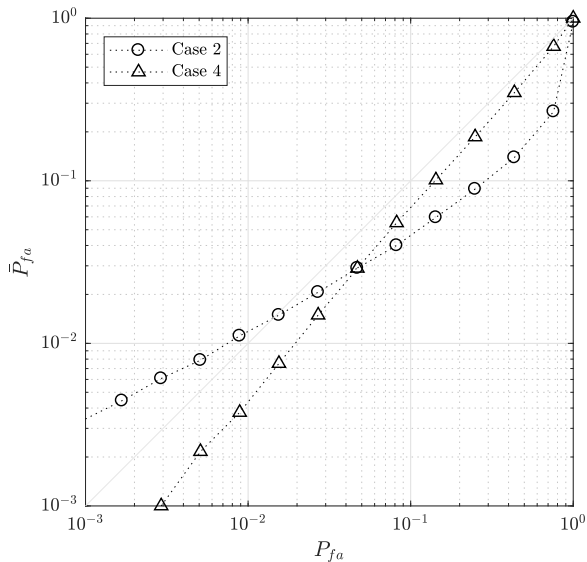
Fig. 7. P_{fa} versus $\bar{P}_{\text{fa}}$ for Cases 2 and 4. When P_{fa} is less than approximately 0.015, then $\bar{P}_{\text{fa}}$ exceeds the constraint for Case 4. Meanwhile, Case 4 remains within the constraint for all P_{fa}.

using MME detection. However, the spectral characteristics of the Wishart distribution are no longer valid in deriving a threshold. Indeed, the correlation across columns may lead to a rather complicated derivation for the distribution of the eigenvalues in the overlapping columns case, although it may be possible to simplify the derivation by using an a shifted gamma distribution as an approximation [13].

Furthermore, it has been shown in Figs. 7-8 that when using the newly proposed test statistic, the limiting distribution threshold results in an empirical false alarm rate within the constraint set by the test, while the semi-asymptotic distribution exceeds this constraint for $P_{\text{fa}} < 0.015$. For $P_{\text{fa}} < 0.05$, the semi-asymptotic threshold has a higher detection rate than the limiting distribution threshold, while the opposite is true for $P_{\text{fa}} > 0.05$. Therefore, when using the test statistic proposed in this paper, the preferred choice of threshold depends on the values of the test parameters.

REFERENCES

[1] S. Haykin, "Cognitive Radio: Brain-Empowered Wireless Communications," *IEEE Journal on Selected Areas in Communications*, vol. 23, no. 2, 2005, pp. 201-220.
[2] S. K. Jayaweera, *Signal Processing for Cognitive Radios*. Hoboken, NJ: John Wiley and Sons, Inc., 2015.
[3] Y. Zeng and Y.-C. Liang, "Maximum-Minimum Eigenvalue Detection for Cognitive Radio," *2007 IEEE 18th International Symposium on Personal, Indoor and Mobile Radio Communications*, Athens, 2007, pp. 1-5.
[4] F. Penna *et al.*, "Cooperative spectrum sensing based on the limiting eigenvalue ratio distribution in Wishart matrices'," *IEEE Comm. Lett.*, vol. 13, no. 7, pp. 507-509, 2009.
[5] R. J. Muirhead, *Aspects of Multivariate Statistical Theory*. New York: John Wiley and Sons Inc., 1982.
[6] Z. D. Bai, "Methodologies in spectral analysis of large dimensional random matrices, a review," *Statistica Sinica*, vol. 90, pp. 611-677, 1999.
[7] C. Tracy and H. Widom, "On orthogonal and symplectic matrix ensembles," *Comm. Math. Phys.*, vol. 177, pp. 727-754, 1996.

[8] I. M. Johnstone, "On the distribution of the largest eigenvalue in principle components analysis," *The Annals of Statistics*, vol. 29, no. 2, pp. 295-327, 2001.
[9] O. N. Feldheim and S. Sodin, "A universality result for the smallest eigenvalues of certain sample covariance matrices," *Geom. Funct. Anal.*, vol. 20, no. 1, pp. 88-123, 2010.
[10] R. Vershynin, "Introduction to the non-asymptotic analysis of random matrices," in *Compressed Sensing, Theory and Applications*, Y. C. Eldar and G. Kutyniok, Eds. Cambridge, UK: Cambridge University Press, pp. 210-268, 2012.
[11] A. Ahmed *et al.*, "Spectrum Sensing based on Maximum Eigenvalue Approximation in Cognitive Radio Networks," *2015 IEEE 16th International Symposium on a World of Wireless, Mobile and Multimedia Networks*, Boston, 2015, pp. 1-6.
[12] A. V. Oppenheim *et al.*, *Signals and Systems*. New York: Pearson, 1996.
[13] M. Chiani, "Distribution of the largest eigenvalue for real Wishart and Gaussian random matrices and a simple approximation for the Tracy-Widom distribution," *Journal of Multivariate Analysis*, vol. 129, pp. 69-81, 2014.

(a)

(b)
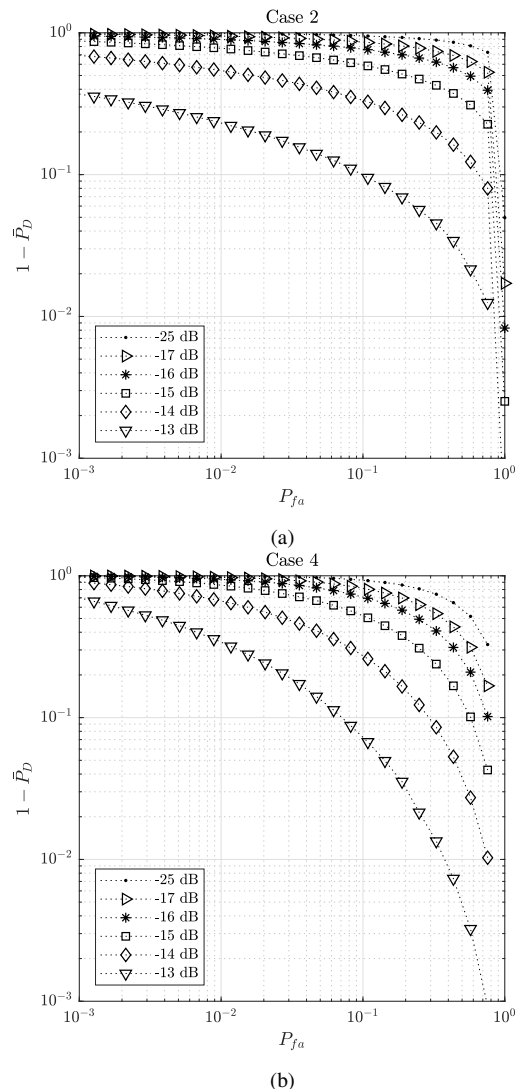
Fig. 8. a) Complementary ROC curves for Case 2. b) Complementary ROC curves for Case 4. There is a trade-off in performance between the two thresholds, dependent on the selected value of P_{fa}. Case 2 has a higher detection probability than Case 4 for $P_{\text{fa}} < 0.05$, while Case 4 has the higher detection probability for $P_{\text{fa}} > 0.05$.